JOURNAL OF BACTERIOLOGY, Apr. 2011, p. 1533–1542 Vol. 193, No. 7
0021-9193/11/$12.00 doi:10.1128/JB.01100-10

The MreB-Like Protein Mbl of *Streptomyces coelicolor* A3(2) Depends on MreB for Proper Localization and Contributes to Spore Wall Synthesis▽†

Andrea Heichlinger,[1] Moritz Ammelburg,[2] Eva-Maria Kleinschnitz,[1] Annette Latus,[1] Iris Maldener,[3] Klas Flärdh,[4] Wolfgang Wohlleben,[1] and Günther Muth[1]*

Interfakultäres Institut für Mikrobiologie und Infektionsmedizin Tübingen IMIT, Mikrobiologie/Biotechnologie, Eberhard Karls Universität Tübingen, Auf der Morgenstelle 28, 72076 Tübingen, Germany[1]; Abteilung 1, Proteinevolution, Max-Planck-Institut für Entwicklungsbiologie, Spemannstr. 35, 72076 Tübingen, Germany[2]; Interfakultäres Institut für Mikrobiologie und Infektionsmedizin Tübingen IMIT, Organismische Interaktionen, Eberhard Karls Universität Tübingen, Auf der Morgenstelle 28, 72076 Tübingen, Germany[3]; and Department of Biology, Lund University, Sölvegatan 35, 22362 Lund, Sweden[4]

Received 15 September 2010/Accepted 23 December 2010

Most bacteria with a rod-shaped morphology contain an actin-like cytoskeleton consisting of MreB polymers, which form helical spirals underneath the cytoplasmic membrane to direct peptidoglycan synthesis for the elongation of the cell wall. In contrast, MreB of *Streptomyces coelicolor* is not required for vegetative growth but has a role in sporulation. Besides MreB, *S. coelicolor* encodes two further MreB-like proteins, Mbl and SCO6166, whose function is unknown. Whereas MreB and Mbl are highly similar, SCO6166 is shorter, lacking the subdomains IB and IIB of actin-like proteins. Here, we showed that MreB and Mbl are not functionally redundant but cooperate in spore wall synthesis. Expression analysis by semiquantitative reverse transcription-PCR revealed distinct expression patterns. *mreB* and *mbl* are induced predominantly during morphological differentiation. In contrast, *sco6166* is strongly expressed during vegetative growth but switched off during sporulation. All genes could be deleted without affecting viability. Even a Δ*mreB* Δ*mbl* double mutant was viable. Δ*sco6166* had a wild-type phenotype. Δ*mreB*, Δ*mbl*, and Δ*mreB* Δ*mbl* produced swollen, prematurely germinating spores that were sensitive to various kinds of stress, suggesting a defect in spore wall integrity. During aerial mycelium formation, an Mbl-mCherry fusion protein colocalized with an MreB-enhanced green fluorescent protein (MreB-eGFP) fusion protein at the sporulation septa. Whereas MreB-eGFP localized properly in the Δ*mbl* mutant, Mbl-mCherry localization depended on the presence of a functional MreB protein. Our results revealed that MreB and Mbl cooperate in the synthesis of the thickened spore wall, while SCO6166 has a nonessential function during vegetative growth.

The peptidoglycan (PG) layer, consisting of long glycan strands cross-linked by short peptides, is a major determinant of bacterial cell shape (51). Most species with a complex, nonspherical morphology contain the actin-like MreB protein, which belongs to the HSP70-actin-sugar kinase (ASHKA) superfamily of proteins (4, 48). MreB was shown to polymerize into a dynamic helical filament underneath the cytoplasmic membrane spanning the long axis of the cells (11, 17, 25, 30, 33). In rod-shaped bacteria, MreB is thought to interact with other proteins to position a cell wall-synthesizing complex at the lateral cell wall (16, 17, 32). The incorporation of new PG at the lateral wall results in cell elongation, thus determining rod-shaped morphology. Gram-negative bacteria seem to have a single *mreB* gene, usually in an operon with *mreC* and *mreD*. Gram-positive bacteria often encode three MreB-like proteins that show a considerable degree of similarity (>50%). All three *mreB* homologues of *Bacillus subtilis*, *mreB*, *mbl*, and *mreBH*, have an important role in cell shape determination. Whereas *mreB* and *mbl* are essential under normal growth conditions and mutants could survive only after supplementation with 3 mM Mg^{2+} (18, 25, 27), *mreBH* inactivation was less severe (8). *B. subtilis* mutants that are depleted for or defective in a single MreB homologue differed slightly in their phenotype. *mreB* mutants were straight with an increased diameter, suggesting that MreB controls cell width. *mbl* mutants were twisted, indicating that Mbl controls the linear axis (27). MreBH probably regulates autolytic activity, since it interacts with the cell wall hydrolase LytE (8). Nevertheless, the three *mreB* homologues are able to partially complement the defects of the single mutants when overexpressed (27, 44). Also, the three MreB homologues colocalize to the same helical structure in the cell (7, 8). From the phenotype of the mutants and the localization pattern, it was concluded that the three MreB homologues in particular were required to maintain growth and cell shape under stress conditions (27). Besides positioning the lateral wall-synthesizing complex, the MreB cytoskeleton seems to be involved in many other cellular processes, such as the positioning of the DNA replication machinery for proper

* Corresponding author. Mailing address: Interfakultäres Institut für Mikrobiologie und Infektionsmedizin Tübingen IMIT, Mikrobiologie/Biotechnologie, Eberhard Karls Universität Tübingen, Auf der Morgenstelle 28, 72076 Tübingen, Germany. Phone: 4970712974637. Fax: 497071295979. E-mail: gmuth@biotech.uni-tuebingen.de.

† Supplemental material for this article may be found at http://jb.asm.org/.

▽ Published ahead of print on 21 January 2011.

TABLE 1. Strains and plasmids

Strain/plasmid	Relevant characteristic(s)	Reference or source
E. coli Xl1 blue	F′::Tn*10 proA*$^+$*B*$^+$ *lacI*^{q} *supE44* Δ(*lacZ*)M15 *hsdR17 recA1 endA1 gyrA96 thi-1 relA1*	5
E. coli ET 12567	GM2929 *zjj*-202, mutant *hsdM*, mutant *hsdR*	36
E. coli BTH101	F$^-$ *cya-99 araD139 galE15 galK16 rpsL1* (Str^r) *hsdR2 mcrA1 mcrB1*	26
E. coli BW 25113/pIJ790	Δ(*araD-araB*)*567* Δ*lacZ4787*(::*rrnB-4*) *lacIp-4000*(*lacI*^{q}) λ^{-1} *rpoS369*(*Am*) *rph-1* Δ(*rhaD-rhaB*)*568 hsd514*; pIJ790:[*oriR101*] [*repA101*(ts)] *araBp-gam-beta-exo*	21
S. coelicolor M145	Prototrophic, SCP1$^-$ SCP2$^-$	29
Δ*mreB*	*mreB* replacement mutant of M145 (*mreB-IFD*)	37
Δ*mreB*::pPM6 [mreB-IFDc]	*mreB* replacement mutant of M145 (*mreB-IFD*) complemented by the integration of pPM6, *aac*	37
Δ*mbl*	*mbl* replacement mutant of M145	Present study
Δ*mreB* Δ*mbl*	*mreB* replacement mutant of M145, *mbl* replaced by an *aac* cassette	Present study
Δ*sco6166*	*sco6166* replacement mutant of M145	Present study
Δ*pbp2*	*pbp2* replacement mutant of M145	Kleinschnitz et al., unpublished
Δ*mreB*::pPM4 [SCPM6]	*mreB* replacement mutant of M145 (*mreB-IFD*), complemented by the integration of pPM4, *aac*	37
Δ*pbp2*::pPM4	*pbp2* replacement mutant of M145 with integration of pPM4, *aac*	Present study
Δ*mbl*::pPM4	*mbl* replacement mutant of M145 with integration of pPM4, *aac*	Present study
M145::pAH5	pK18-*mbl-mcherry* integrated into *mbl* of M145, *aphII*	Present study
Δ*mreB*::pAH5	*mreB* replacement mutant of M145 (*mreB-IFD*), with pAH5 integrated into *mbl*, *aphII*	Present study
Δ*pbp2*::pAH5	*pbp2* replacement mutant of M145 with integration of pAH5, *aphII*	Present study
pK18	*aphII*, *lacZ*α	40
C24	*aphII*, *S. coelicolor* chromosomal fragment encoding SCO2431-SCO2461	41
pTST101	*bla*, *malE-egfp* fusion	J. Altenbuchner, personal communication
pTST101-mcherry	*bla*, *malE-mcherry* fusion	G. Muth, unpublished
pPM4	pSET152 derivative, *mreB-egfp* fusion	37
pUZ8002	*aphII*, RP4 transfer region	29
pCP20	[*repA101*(ts)], *bla*, *frt*	9
pIJ773	*bla*, *aac*, *oriT*	21
pKT25	*aph*, *cya*-T25	26
pUT18c	*bla*, *cya*-T18	26
pKO6166	pK18 derivative, *aphII*, *sco6166* deletion vector	Present study
pAH4	pK18, *aphII*, *mbl-egfp* fusion	Present study
pAH5	pK18, *aphII*, *mbl-mcherry* fusion	Present study
M145::pAH5-pPM4	pAH5 integrated into *mbl* of M145, integration of pPM4, *aphII*, *aac*	Present study
pGM202-Mbl	pGM190 derivative, *aphII*, *tsr*, P_{tipA}, encoding a Mbl-His_6 fusion protein	Present study

chromosome segregation during cell division and localizing other proteins to distinct sites (12, 13, 14, 28, 34).

In contrast to the rod-shaped bacteria that depend on MreB proteins to control their cell wall assembly, many Gram-positive bacteria of the phylum *Actinobacteria* grow in a different way by building their cell walls at the cell poles (10). Corynebacteria and mycobacteria do not contain *mreB* genes, yet they acquire rod shape by polarized growth, and this depends on the coiled-coil protein DivIVA (35). Similarly, streptomycetes do not divide by binary fission and grow by apical tip extension to form a multiply branching mycelium (22).

Against this background, it was a surprise that an *mreB* cluster is present in *S. coelicolor* (6). It was later shown that *mreB* was dispensable for the apical growth of vegetative hyphae, and loss affected the assembly of the spore wall (37). However, like *B. subtilis*, *S. coelicolor* encodes three MreB homologous proteins, MreB (SCO2611), Mbl (SCO2451), and SCO6166, and it could not be excluded that the dispensability of MreB for vegetative growth was due to some redundancy among these proteins. In this work, we characterized the role of the three *S. coelicolor* MreB-like proteins. We analyzed their expression profile, generated mutants, and localized Mbl and MreB fusion proteins in the wild-type and different mutant backgrounds. We report that the three MreB homologues of *S. coelicolor* have clearly different functions. Whereas MreB and Mbl cooperate in spore wall synthesis, SCO6166 has a nonessential function during vegetative growth.

MATERIALS AND METHODS

Bacterial strains and media. Strains and plasmids used in this study are listed in Table 1. *S. coelicolor* strains were cultivated on mannitol soya flour (MS) agar plates or in S medium (29). The cultivation of strains and procedures for DNA manipulation were performed as previously described for *Escherichia coli* (43) and *S. coelicolor* (29). Oligonucleotides used for reverse transcription-PCR (RT-PCR) and subcloning are given in Tables 2 and 3, respectively.

Inactivation of *mbl* and *sco6166*. Mbl was deleted by the PCR targeting (21) of cosmid C24 (41). Following the λ red-mediated replacement of *mbl* by a PCR-amplified *aac(3)IV* cassette (primer pair mblredup/mblredrev), the resulting cosmid, C24-aac, was introduced into M145 by intergeneric conjugation, and an *mbl* replacement mutant, Δ*mbl-aac* (double crossover), was selected.

Subsequently, the *aac(3)IV* cassette was deleted from cosmid C24-aac by FLP recombination target (FRT) recombination using *E. coli* BT340 (9), and the resulting cosmid was introduced into the *S. coelicolor* mutant Δ*mbl-aac*. Finally, apramycin-sensitive Δ*mbl* colonies were selected in which *mbl* was replaced by a remaining 81-bp scar sequence. The Δ*mreB* Δ*mbl* double mutant was generated by introducing cosmid C24-aac in the Δ*mreB* mutant (37) and screening for

TABLE 2. Oligonucleotide primers used for RT-PCR

Primer	Sequence (5′→ 3′)	Fragment size (bp)
RThrdBleft3	GGTCGAGGTCATCAACAAGC	205
RThrdBrig3	CTCGATGAGGTCACCGAACT	
RT-mreBf	GGGGAACTCAATGTCGTTCA	174
RT-mreBr	CCGATCATCTTCTTCGCTTC	
RT-mblleft4	CATGCTGCGTCATCTGCT	172
RT-mblright4	GATGAGCGTGTCGACGAGT	
RT-6166f	ATCTCACGGAGGTGGTGCT	140
RT-6166r	AGCATCGAGGTCGTCATGT	

TABLE 3. Oligonucleotides used for cloning experiments

Primer	Sequence[a] (5′→3′)
Ecoupfw	AAGAATTCTGATCTCCTGCGCCTG
uprchBgBc	TCATGATCAGATCTCACGGTCATCGTCCG
loupchBcBg	GTGAGATCTGATCATGATCCGGTACCGGG
Hlorev	GGAAGCTTGACAGCGTGAGAGAC
mblupNde	GGCATATGACCGCCAGTACTG
mblloBg-gfp	GGAGATCTGTCGGAGTCGGCGTG
6166upNde	GGCATATGACCGTGCTCCGG
6166loBg	CCAGATCTGTGCGGGTGGGTGTC
mblredup	GGCCCCGCACGGTCCGCGCTCTCGGGAG GATTCGCCATG GATATCATTCCGGGGA TCCGTCGACC
mblredrev	TGCGTCAGGCTTCCCCGGTCGCCGCCCGG CGGCGGATCA GATATCTGTAGGCTGGA GCTGCTTC
loupchBcBg	GTGAGATCTGATCATGATCCGGTACCGGG
Hlorev	GGAAGCTTGACAGCGTGAGAGAC
CHSTEup2	AGGATTCGCCATGGAATTCCACGCCGACT CCGACTG
HKHrev2	CCAAGCTTGGCGGTCGGGTGCAGG
mreBXba	AATCTAGAGAACGACATTGAGTTC
mreBK	TCGGTACCGATCTACGGGGCGAGGC
mblXba	AATCTAGAGTATTGGCAGTACTG
mblK	CTGGTACCCAGTCGGAGTCGGCGTG
6166Xba	ACTCTAGAGACCGTGCTCCGGCGG
6166K	AAGGTACCCAGTGCGGGTGGGTGTC
rodZXba	ACTCTAGAGTCCAACGGCAAATCC
rodZK	TTGGTACCCATCCGACCTGCGGGT
mreCXba	ACTCTAGAGAGGGACACGAAAGAG
mreCK	AAGGTACCACGGCTCGGGCTGCTC
mreDXba	ACTCTAGAGCGCGTCAACCGGATC
mreDK	AAGGTACCACAGCCGCTTGACCCC
pbp2Xba	ACTCTAGAGACCAACATCCCCGAG
pbp2K	AAGGTACCATACGCGGTGCCCTCC
sfrXba	ACTCTAGAGACCGGCAACAGCTTC
sfrK	AAGGTACCACGCCGACATCGGTCT

[a] Restriction sites are underlined.

apramycin-resistant and kanamycin-sensitive colonies. Note that the Δ*mreB* Δ*mbl* mutant still contains the *aac(3)IV* gene.

To delete *sco6166*, a 1.6-kb upstream fragment (primer pair Ecoupfw/uprch-BgBc), including the start codon of *sco6166*, and a 1.6-kb downstream fragment (primer pair loupchBcBg/Hlorev), including the *sco6166* stop codon, were amplified by PCR and cloned into pK18, yielding pKO1666. After the transformation of M145 and the integration of the deletion vector pKO6166 by a single crossover (kanamycin resistant), an *sco6166* mutant was isolated by selecting for the second crossover (kanamycin sensitive). Correct gene replacement was confirmed by PCR analyses and Southern blotting. Hybridization probes were amplified with primers CHSTEup2/HKHrev2 and loupchBcBg/Hlorev.

Construction of *gfp* and *mcherry* fusions. To construct a C-terminal fusion with the enhanced green fluorescent protein (eGFP) or mCherry protein, *mbl* and *sco6166* genes were amplified using the primers mblupNde/mblloBg-gfp and 6166upNde/6166loBg, respectively, cut with NdeI and BglII, and fused to the *egfp* or *mcherry* gene in plasmids pTST101 (J. Altenbuchner, personal communication) or pTST101mCherry (G. Muth, unpublished data) cut with NdeI and BamHI. The resulting fusion genes were cut from pTST101 and cloned in the nonreplicative vector pK18, generating pK18-Mbl-eGFP (pAH4), pK18-Mbl-mCherry (pAH5), and pK18-6166-mCherry. The plasmids then were integrated into chromosomal *mbl* or *sco6166* genes of *S. coelicolor* M145 via homologous recombination.

For colocalization experiments, the plasmid pPM4 (37), carrying an *mreB-egfp* fusion gene, was integrated into the ΦC31 *att* site of M145::pAH5.

RNA extraction. Total RNA was isolated from wild-type M145 grown for 48 and 72 h on LB agar or 48, 72, and 96 h on MS agar overlaid with cellophane discs. Cells were harvested, resuspended in RNAprotect bacteria reagent (Qiagen), centrifuged, and resuspended in Tris-EDTA (TE) buffer. Cell disruption was performed with glass beads (0.45 to 0.5 mm) and a Precellys homogenizer from Peqlab (for substrate mycelium, 2× 6,500 rpm for 30 s; for aerial mycelium and spores, 4× 6,500 rpm for 30 s). RNA was isolated with an RNeasy kit from Qiagen as described previously (46). The RNA samples were resuspended in H_20 and quantified spectrophotometrically at 260 nm with a Nanodrop photometer (Peqlab). All RNA isolates had an optical density at 260 nm (OD_{260})/OD_{280} ratio between 1.8 and 2.0, indicating clean RNA isolates. The RNA quality also was checked by 1.0% agarose gel electrophoresis and ethidium bromide staining. To exclude the contamination of the RNA with DNA, a control PCR was done with primers for the housekeeping gene *hrdB* (RNA polymerase principal sigma factor HrdB; SCO5820).

Semiquantitative RT-PCR analysis. A two-step semiquantitative RT-PCR method was used to measure gene expression during the morphological differentiation of M145. RNA was isolated from two independently grown cultures, and RT-PCR was repeated twice. cDNA synthesis was performed as described in reference 46 using 3 μg of RNA. Sixty ng of cDNA was used for RT-PCR. The housekeeping gene *hrdB* was used as an internal control. The optimal PCR annealing temperature of all primers was 62°C. Primer sequences are listed in Table 2. PCRs were performed with the Bio-Rad MJ mini personal thermal cycler using 60 ng of cDNA, 400 nM each primer, 200 μM deoxynucleoside triphosphates (dNTPs), 1× polymerase buffer (Qiagen), and 1 U *Taq* polymerase (Qiagen) in a 25-μl volume. All reactions were done with the same program: 95°C for 2 min, and then 28 cycles of 95°C for 1 min, 62°C for 1 min, and 72°C for 30 s, followed by an additional 7-min extension step at 72°C. The RT-PCR samples were loaded on a 2% agarose gel and stained with ethidium bromide.

Bacterial two-hybrid analyses. To detect protein interactions, respective *S. coelicolor* genes were amplified with primers (listed in Table 3) containing XbaI and KpnI sites. Subsequently, PCR fragments were cloned as XbaI/KpnI fragments into plasmids pKT25, pUT18, and pUT18c to generate translational fusions with the catalytic domains of the *Bordetella pertussis* adenylate cyclase (26). The *E. coli cya* mutant BTH101 was cotransformed with pUT18c and pKT25 derivatives and spotted on 5-bromo-4-chloro-3-indolyl-β-D-galactopyranoside (X-Gal) plates. The ability of cotransformants to metabolize X-Gal, resulting in blue color, is based on a functional adenylate cyclase due to the interaction of the fusion proteins.

Phase-contrast microscopy. For light and fluorescence microscopy of substrate mycelium, aerial mycelium and spore chains cultures were plated on MS agar, and sterile coverslips were inserted at a 45° angle into the agar. Coverslips were removed after 2 to 4 days of incubation at 30°C and mounted on slides coated with phosphate-buffered saline (PBS) with 1% agarose. For the phenotypic characterization of the mutants, pictures were taken with an Olympus system microscope BX60 equipped with an F-view II camera (Olympus). Fluorescent microscopy was done with a Zeiss DM5500B microscope equipped with a Leica DFC360FX camera.

For colocalization studies, the samples were viewed using a Zeiss Axio Imager.Z1 microscope equipped with X-Cite 120 illumination (EXFO Photonic Solution, Inc.), and images were captured and processed using a 9100-02 electron multiplier charge-coupled device camera (Hamamatsu Photonics) and Volocity 3DM software (Improvision).

Spore size measurements. The wild-type M145 and the mutants Δ*mbl*, Δ*mreB* Δ*mbl*, and Δ*sco6166* were inoculated on MS agar. Coverslips were inserted and removed after 4 days of inoculation and observed with an Olympus system BX60 microscope. Average values (length and width, in μm) of 200 spores of M145, Δ*mbl*, Δ*mreB*, Δ*mreB* Δ*mbl*, Δ*sco6166*, and Δ*mbl*(pGM202-Mbl) were measured with AnalySIS software (Olympus).

Transmission electron microscopy. *S. coelicolor* strains were grown on MS agar for 5 days. Spores were harvested and fixed with 2% glutaraldehyde, embedded in 2% agarose, and treated with 1% OsO_4 in 0.1 M phosphate buffer on ice for 30 min. Subsequently, the samples were dehydrated with increasing concentrations of ethanol, infiltrated by ethanol:EPON (2:1 to 1:2 ratio), and

embedded in pure EPON. Ultrathin sections were stained with uranylacetate and lead citrate. The samples were examined with a Phillips Tecnai electron microscope at 80 kV.

Analyses of heat, salt, lysozyme, and vancomycin resistance. Heat resistance was assayed by incubating spores (10^6/ml) for 30 min at 30 and 60°C. Subsequently, 5 μl of the spore samples was spotted onto LB agar and incubated for 3 days at 30°C. To analyze salt resistance, serial dilutions (H_2O) of spore suspensions (titer, 10^8 to 10^9/ml) were plated on LB agar with 6 and 0.5% NaCl, respectively. Plates were cultivated for 2 days at 30°C. The survival rate was calculated as the percentage of the colony titer on plates with 6% NaCl divided by the titer on plates with 0.5% NaCl. Resistance to cell wall-damaging agents was assayed by plating spores (10^5) of the different mutants and the wild type on LB agar and applying filter discs containing 50 μg lysozyme or 5 μg vancomycin. Plates were inoculated for 2 days at 30°C before being photographed.

Bioinformatic analyses. HHpred (45), a remote homology detection method based on the comparison of profile-hidden Markov models, was used to search the Protein Data Bank (PDB) (3) for homologues of known structure. Searches with MreB and Mbl from *S. coelicolor* retrieved the rod shape-determining protein MreB from *T. maritima* (PDB accession no. 1jce) (48) as the closest homolog of known structure. For the MreB-like protein SCO6166, the ethanol utilization protein EutJ from *Carboxydothermus hydrogenoformans* (3h1q) had the highest score.

Homology models of the three MreB-like proteins of *S. coelicolor* were generated by Modeler (42) using HHpred alignments to the best hit as a template. The models were superimposed interactively in Swiss-PDB Viewer (20). Molecular structures were rendered in PyMol (www.pymol.org).

RESULTS

***S. coelicolor* has three *mreB*-like genes.** *S. coelicolor* contains three genes encoding MreB-like proteins. *mreB* is located in a cluster with the other rod shape-determining genes *mreC*, *mreD*, *pbp2*, and *sfr* (6). The second *mreB* homologue, *mbl*, lies between two genes encoding protein kinases. MreB and Mbl have sizes of 36.5 and 37.5 kDa, respectively, show a similarity of 42% (identical amino acids), and can be aligned over the whole length (Fig. 1A). In contrast, the third MreB-like protein, SCO6166, is shorter and has a molecular size of 28.7 kDa. *sco6166* is translationally coupled to *sco6165*, encoding a 121-amino-acid (aa) protein homologous to the DnaK suppressor DksA of *E. coli* and TR: O83134 (EMBL:AE001194) from *Treponema pallidum*. The modeling of SCO6166 on the template of *Thermotoga maritima* MreB showed that SCO6166 lacks the subdomains IB and IIB of actin-like proteins (Fig. 1B). Whereas homologues of MreB and Mbl are present in all streptomycetes, some strains, such as *S. avermitilis* (NC_003155.4) or *S. viridochromogenes* (NZ_ACEZ00000000), do not contain a homologue of SCO6166, indicating a nonessential function for SCO6166.

The three *mreB*-like genes have different expression profiles. Previous S1 mapping experiments identified three promoters upstream of *mreB*, one strongly induced during the morphological differentiation of *S. coelicolor* (6). To characterize the expression profile of the other *mreB* homologues, we performed semiquantitative RT-PCR experiments with RNA isolated from surface-grown cultures at different time points (Fig. 2). After 48 and 72 h on LB agar, when only substrate mycelium was formed, *mreB* was expressed but a *mbl* transcript could not be detected; *sco6166* showed the strongest expression. This was in agreement with detailed microarray data from *S. coelicolor* liquid cultures (38) showing the strong expression of *sco6166*, intermediate expression of *mreB*, and only very weak expression of *mbl* during a period of 40 h (K. Nieselt, personal communication). After 48 h on MS agar, when aerial mycelium already was developed, *mreB* transcription increased and *mbl* transcription was detectable at a low level. In contrast, *sco6166* expression strongly decreased (Fig. 2). After 72 and 96 h on MS agar, when spore chains have been formed in the aerial mycelium, the transcription of both *mreB* and *mbl* further increased, while *sco6166* expression was no longer detectable. The expression profile suggested a role for *mreB* and *mbl* in sporulation, whereas the third *mreB*-like gene, *sco6166*, seems to have a function in vegetatively growing mycelium.

A Δ*mreB* Δ*mbl* double mutant is viable. In contrast to *B. subtilis*, where *mreB* and *mbl* are essential under normal growth conditions and mutants require high concentrations of Mg^{2+} for survival (18, 25), the inactivation of *mreB* in *S. coelicolor* was tolerated (37). The phenotype of the Δ*mreB* (*mreB-IFD*) mutant suggested a defect in spore wall synthesis. To analyze whether the other *mreB*-like proteins also are involved in spore wall synthesis, we inactivated *mbl* and *sco6166*. *mbl* was replaced by PCR targeting as described in Materials and Methods and in Fig. S1 in the supplemental material, while *sco6166* was deleted from the chromosome by homologous recombination using a nonreplicative deletion vector (see Fig S2). We also deleted *mbl* in the Δ*mreB* mutant (37), generating a Δ*mreB* Δ*mbl* double mutant. All mutants were isolated readily, demonstrating that none of the *mreB* homologues had an essential role for viability. Even the growth of the Δ*mreB* Δ*mbl* double mutant was not affected under standard growth conditions.

Δ*mbl* and Δ*mreB* Δ*mbl* had phenotypes very similar to that of the Δ*mreB* mutant, with swollen, prematurely germinating spores (Fig. 3). Whereas *S. coelicolor* M145 spores had a size of 1.28 by 0.71 μm, Δ*mbl* and Δ*mbl* Δ*mreB* spores were 1.72 by 0.95 and 1.7 by 1.15 μm, respectively (Table 4). The mutant phenotype was more severe when the mutants were grown on MS agar supplemented with 10.3% sucrose, as also reported for *ftsI* and *ftsW* mutants (2). Under these conditions, Δ*mreB*, Δ*mbl*, or Δ*mreB* Δ*mbl* did not sporulate (see Fig. S3 in the supplemental material). Microscopic analyses showed that large areas of the aerial mycelium lysed, and aberrant spore-like particles were formed (Fig. 3B).

By immunogold labeling, MreB has been localized to the inner spore wall, suggesting a role in spore wall synthesis (37). This was confirmed by electron microscopic images showing aberrant Δ*mreB* spores whose spore wall integrity was affected. To demonstrate the involvement of Mbl in spore wall synthesis, we performed electron microscopic studies. These images clearly revealed a distorted spore wall (see Fig. S4 in the supplemental material). Whereas M145 formed uniform round or ellipsoid spores with a confined outer layer, the Δ*mbl* spores were more irregular with a very diffuse outer layer (see Fig. S4 in the supplemental material).

Furthermore, the mutant spores were impaired in their resistance to moderate heat (Fig. 4A), 5% SDS (data not shown), and salt stress (Fig. 4C). Whereas about 100% of M145 spores were able to germinate on LB plus 6% NaCl, only 0.001% of Δ*mreB*, 0.003% of Δ*mbl*, and 0.02% of Δ*mreB* Δ*mbl* spores were able to form colonies (mean values from three independent experiments). In contrast, Δ*sco6166* spores were almost as resistant (89.4% survival) to salt stress as the wild type (Fig. 4C). The transformation of the Δ*mbl* mutant with plasmid pGM202-Mbl, which contains an *mbl-his6* fusion gene under the control of the thiostrepton-inducible *tipA* promoter (Table

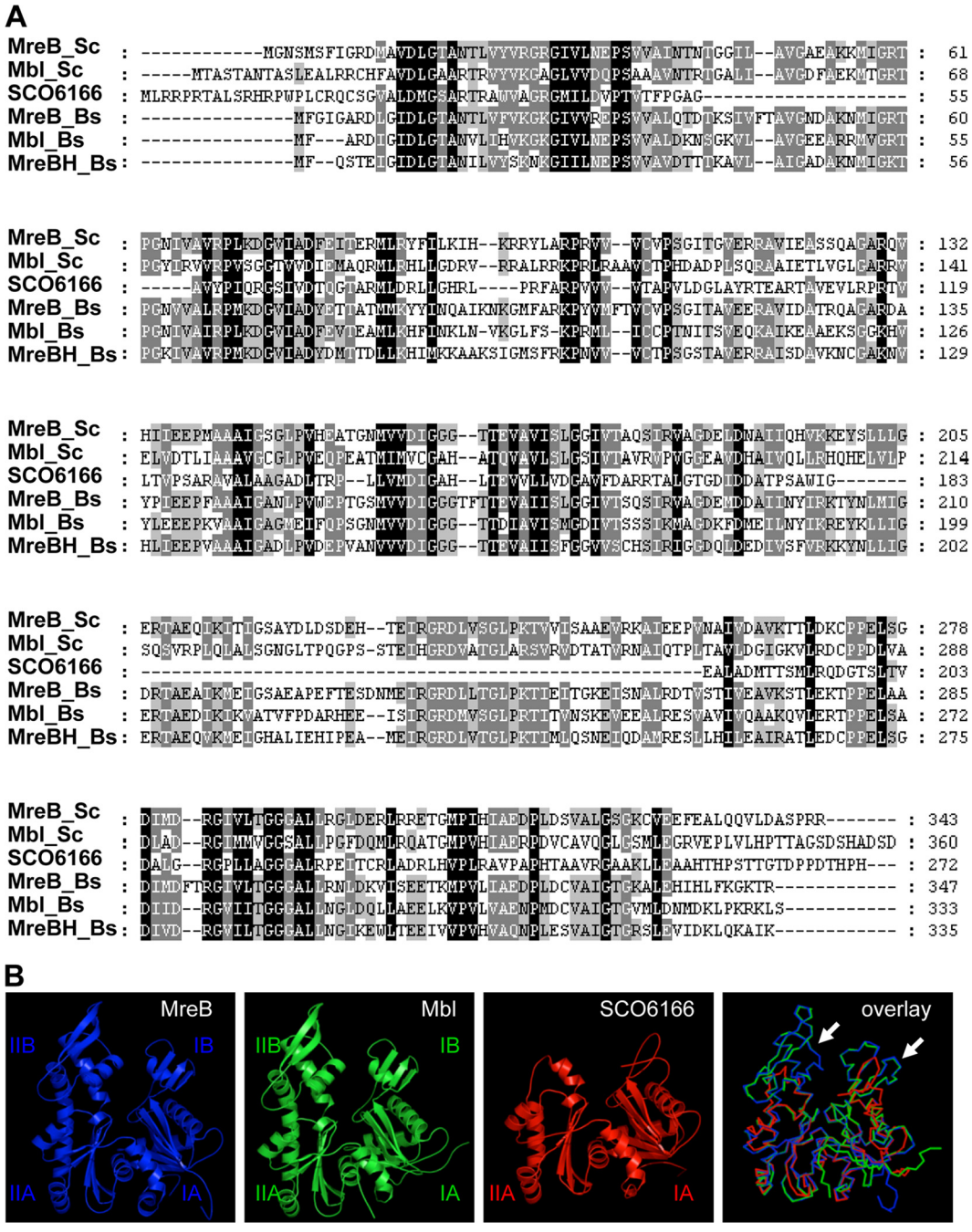

FIG. 1. Similarity of the three *S. coelicolor* MreB homologues. The MreB homologues of *S. coelicolor* and *B. subtilis* were compared by ClustalW sequence alignment (A) and homology modeling (B) using MreB of *Thermotoga maritima* as a template. MreB and Mbl are highly similar to the *B. subtilis* MreB homologues and have an identical structure; SCO6166 lacks subdomains IB and IIB (arrows). The colors in the superposition (lower right panel) correspond to the colors chosen for the individual homology models. MreB is given in blue, Mbl in green, and SCO6166 in red.

1), complemented spore size (Table 4) and heat sensitivity (Fig. 4A), demonstrating that the mutant phenotype was caused solely by *mbl* inactivation.

Since heat and detergent sensitivity is a hallmark for a defective spore wall (37), we studied the effect of lysozyme and vancomycin. Spores of M145 and the mutants were plated onto LB agar, and filter discs soaked with lysozyme or vancomycin were placed on the plates. After incubation at 30°C for 24 h, only very small inhibition zones were formed on M145, Δ*sco6166*, and the Δ*mbl* mutant. However, the Δ*mreB* mutant and the Δ*mreB* Δ*mbl* mutant were much more sensitive, and large inhibition zones were observed (Fig. 4B). If the agar plates were incubated overnight to allow spore germination before the use of the lysozyme or vancomycin discs, no inhibition zones were formed (data not shown), demonstrating that the germinating spores were sensitive but substrate mycelium was resistant.

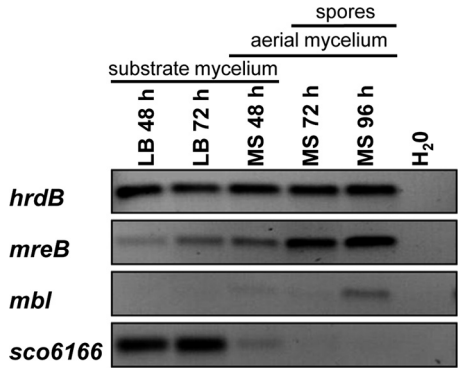

FIG. 2. Transcriptional analysis of the *mreB*-like genes of *S. coelicolor* by semiquantitative RT-PCR. Cultures of *S. coelicolor* M145 were grown on cellophane discs on LB agar or MS agar for different time periods. The stage of morphological differentiation is indicated for the different time points. Following RNA isolation and cDNA synthesis, the amounts of transcripts were compared by PCR. The expression of *hrdB* served as an internal control. The expression of *mreB* and *mbl* increased during morphological differentiation. In contrast, *sco6166* is highly expressed in vegetative mycelia but no longer is transcribed after the onset of sporulation.

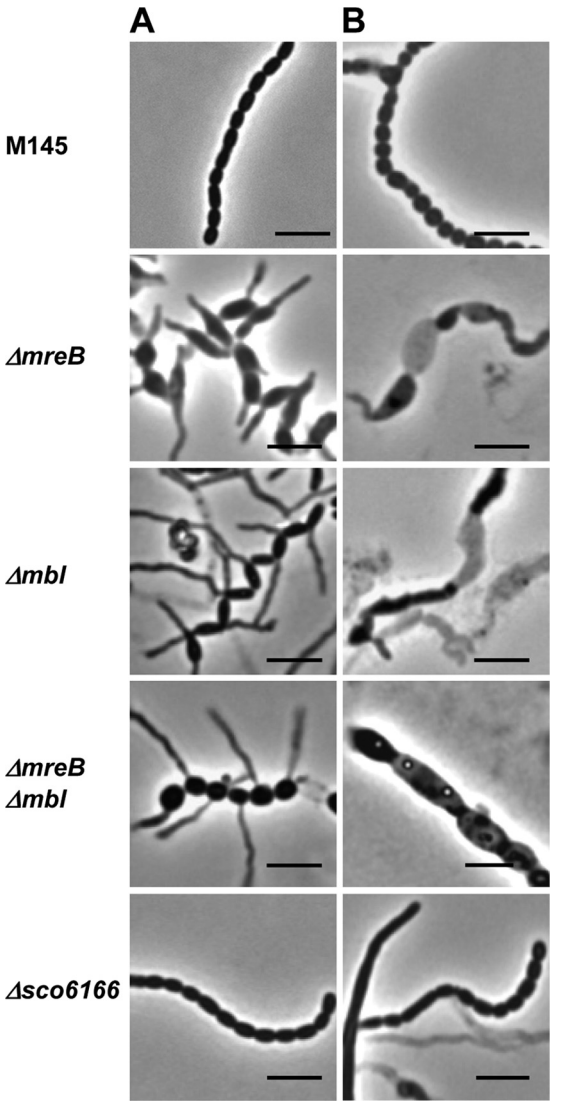

FIG. 3. Aberrant spore phenotype of *S. coelicolor* mutants defective in *mreB*-like genes. Phase-contrast microscopy of spore chains from strains grown for 4 days on MS agar (A) and MS agar plus 10.3% sucrose (B), respectively. Whereas the vegetative mycelium was not affected, Δ*mreB*, Δ*mbl*, and Δ*mreB* Δ*mbl* formed swollen spores (sizes are given in Table 4) that frequently germinate prematurely. In contrast, Δ*sco6166* spores had a wild-type appearance. On MS agar containing 10.3% sucrose, large areas of the aerial mycelium of the Δ*mreB*, Δ*mbl*, and Δ*mreB* Δ*mbl* mutants were lysed, and aberrant spore-like particles were formed (B). Bar, 4 μm.

These mutant phenotypes indicated that *mreB* and *mbl* are involved in spore wall synthesis, with a less important role for *mbl*. In contrast, the Δ*sco6166* mutant behaved like the parent strain M145 in all aspects.

Only MreB, but not Mbl or SCO6166, interacts with RodZ. RodZ, a remarkable multidomain protein that localizes in a helical manner, recently was shown to interact with MreB, probably linking the cytosolic MreB filaments with the membrane-localized lateral wall-synthesizing machinery (1, 49). To analyze the protein-protein interaction of the MreB-like proteins, we used the bacterial two-hybrid system based on the reconstitution of the *Bordetella pertussis* adenylate cyclase (26). The three *S. coelicolor mreB*-like genes, the *rodZ* homologue *sco5751*, and the other genes of the *mre* cluster (*mreC*, *mreD*, *pbp2*, and *sfr*) were fused to the catalytic domains of *cya* and analyzed in cotransformation experiments of the *cya* mutant BTH101 for protein-protein interaction. The MreB homologues were poor interaction partners in these two-hybrid assays, and they did not show the self interaction that would be expected for actin-like proteins. MreB also did not interact with any of the other proteins encoded by the *mre* cluster (data not shown). However, MreB showed a strong interaction with the scaffold protein RodZ (SCO5751). Neither Mbl nor SCO6166 interacted with RodZ or any of the tested fusion proteins (Fig. 5).

MreB and Mbl colocalize during sporulation. An MreB-eGFP fusion protein showed a dynamic localization pattern during morphological differentiation: disperse distribution in substrate mycelium, localization to the sporulation septa in aerial mycelium, and finally the formation of a shell at the inner spore wall (37). To address whether Mbl and SCO6166 had a similar localization pattern, we generated C-terminal fusions of Mbl and SCO6166 with either eGFP or mCherry. The fusion genes were integrated into the chromosome at the original gene locus via homologous recombination. No fluorescence of Mbl-eGFP or Mbl-mCherry was observed in substrate mycelium, probably reflecting the very low *mbl* expression, as demonstrated by RT-PCR. However, in aerial mycelium, Mbl localized to the sporulation septa, like MreB. In young spores, Mbl was found underneath the membrane (Fig. 6A). To prove that Mbl really localizes to the same sites as MreB, we performed colocalization studies by integrating plasmid pPM4 (37), which encodes the MreB-eGFP fusion protein, into the ΦC31 attachment site of M145::pAH5. Mbl-mCherry and MreB-eGFP always colocalized (Fig. 6B).

In contrast, SCO6166-mCherry showed a dispersed fluorescence of the total substrate mycelium without distinct localization patterns (see Fig. S5 in the supplemental material).

TABLE 4. Spore dimensions[a] of *S. coelicolor* and mutants deficient in *mreB* homologous genes

Strain	Length (μm)	Width (μm)
M145	1.28 ± 0.20	0.71 ± 0.07
M145 (pGM190)	1.20 ± 0.15	0.64 ± 0.06
Δ*mreB* [*mreB*-IFD][b]	1.64 ± 0.24	1.16 ± 0.21
Δ*mreB*::pPM6 [IFDc][b]	1.23 ± 0.27	0.84 ± 0.14
Δ*mbl*	1.72 ± 0.38	0.95 ± 0.16
Δ*mbl* (pGM202-Mbl)	1.31 ± 0.18	0.67 ± 0.08
Δ*mreB* Δ*mbl*	1.70 ± 0.33	1.15 ± 0.11
Δ*sco6166*	1.31 ± 0.25	0.78 ± 0.08

[a] $n = 200$.
[b] From reference 38.

Mbl requires MreB for proper localization. To analyze whether MreB and Mbl depend on each other for proper localization, fluorescence generated by MreB-eGFP (pPM4) and Mbl-mCherry (pAH5) (Table 1) was analyzed in a Δ*mreB* or Δ*mbl* background. Mutant Δ*pbp2* (30a) was used as a control, since it showed the same morphological defects, swollen and prematurely germinating spores, as the Δ*mreB* or Δ*mbl* mutant. In Δ*mbl*::pPM4, Δ*mreB*::pPM4, and Δ*pbp2*::pPM4 strains, the characteristic ladder-like fluorescence structure at the sporulation septa of the aerial mycelium (Fig. 7A) and around the spore membrane (see Fig. S6 in the supplemental material) was observed, demonstrating that MreB-eGFP was able to localize independently of Mbl or PBP2.

Whereas Mbl-mCherry localized properly in the Δ*pbp2*::pAH5 strain, no clear Mbl-mCherry foci were observed in the Δ*mreB* mutant (Fig. 7B). RT-PCR analyses demonstrated that the transcription of *mbl-mcherry* was not affected in the Δ*mreB* mutant (see Fig. S7 in the supplemental material). This clearly suggested that Mbl requires MreB for correct localization.

DISCUSSION

Most rod-shaped bacteria achieve their morphology by incorporating new peptidoglycan at the lateral wall in a helical manner (10, 14, 47), probably directed by cytoplasmic MreB filaments (25, 31). Whereas Gram-negative rods require a single MreB homologue for growth and cell shape determination, Gram-positive ones, like *B. subtilis*, depend on three MreB homologues (27, 44). The precise role of the three MreB homologues in directing lateral cell wall growth is not known, and some redundancy has been reported (27).

S. coelicolor is a useful model system to study the role of MreB homologues, since none of the three *mreB*-like genes is essential for viability, demonstrating that they are not involved in vegetative growth by apical tip extension. This provided the unique possibility to analyze the function of the distinct *mreB* homologues in a defined mutant background. The conservation of *mreB* in *Streptomyces* and other sporulating actinomycetes, its mutant phenotype, and its localization to sites where spore wall synthesis occurs demonstrated its role in spore wall synthesis (37). In this report, we provide evidence that Mbl also is involved in sporulation, while the third MreB homologue, SCO6166, has a completely different function. This conclusion is supported by homology modeling, expression analysis, mutant phenotypes, electron microscopy, protein-protein interaction studies, and protein localization experiments.

MreB and Mbl cooperate in the synthesis of a thickened spore wall. The role of *mreB* in directing the synthesis of a thickened spore wall has been reported already (37). There are several lines of evidence that suggest a related function for Mbl. The structure of Mbl, deduced from homology modeling, is nearly identical to that of MreB, indicating a very similar function.

Expression analysis by semiquantitative RT-PCR analysis showed the induction of *mreB* and *mbl* during morphological differentiation. Whereas *mbl* expression was not detectable in substrate mycelium but increased considerably during sporu-

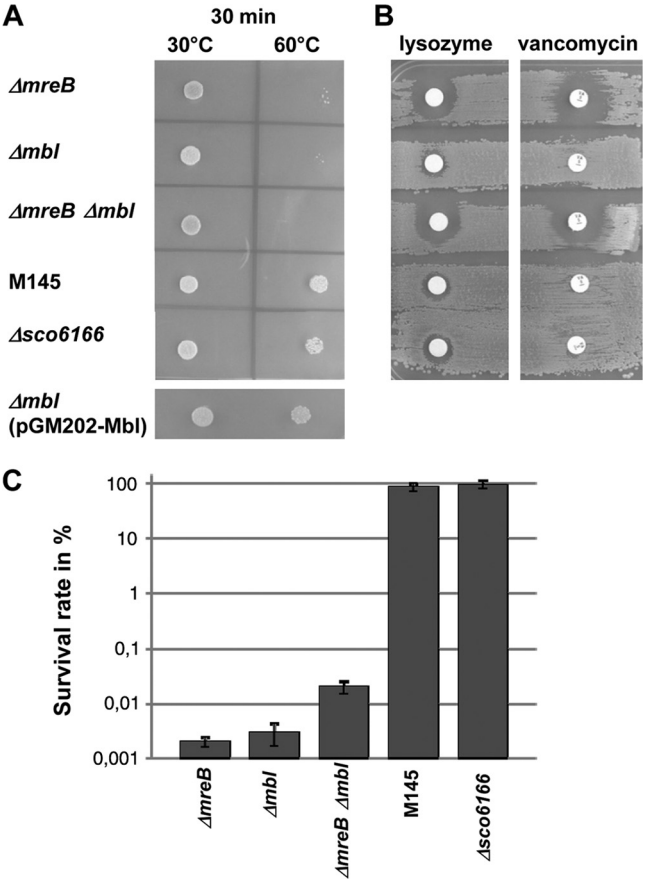

FIG. 4. Sensitivity of mutant spores to moderate heat, cell wall-lytic agents, and salt stress. (A) To assess resistance to moderate heat, spores of M145, Δ*mreB*, Δ*mbl*, Δ*mreB* Δ*mbl*, Δ*sco6166*, and Δ*mbl*(pGM202-Mbl) were incubated for 30 min at 30 or at 60°C, spotted onto LB agar, and incubated for 3 days at 30°C. (B) Resistance to cell wall-lytic agents was studied by plating spores onto LB agar, and filter discs with lysozyme (50 μg) or vancomycin (5 μg) were applied. The growth of M145, Δ*mbl*, and Δ*sco6166* is only slightly affected, while Δ*mreB* and Δ*mreB* Δ*mbl* show large inhibition zones. (C) Survival rates of mutant strains exposed to salt stress. Spore dilutions (in H_2O) were plated on LB agar plates containing 0.5% NaCl or 6% NaCl. The survival rates (mean values of three independent experiments) represent the percentage of colony titer on LB plus 6% NaCl in relation to the titer on LB plus 0.5% NaCl. In contrast to those of M145 and Δ*sco6166*, the spores of Δ*mreB*, Δ*mbl*, and Δ*mreB* Δ*mbl* were impaired in germination and colony formation under high salt concentrations.

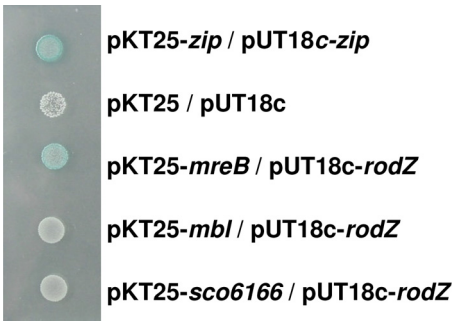

FIG. 5. Bacterial two-hybrid analysis demonstrating the interaction of MreB with the scaffold protein RodZ (SCO5751). *mreB*, *mbl*, *sco6166*, and further morphogenic genes (see Material and Methods for details) of *S. coelicolor* were fused to the functional *cya* domains T25 (pKT25) and T18 (pUT18c) of the *Bordetella pertussis* adenylate cyclase (26). Cotransformants of the *cya* mutant BTH101 were spotted onto X-Gal plates. The blue color indicates the reconstitution of a functional adenylate cyclase due to the interaction of the fusion proteins. MreB, but neither Mbl nor SCO6166, interacted with the *S. coelicolor* RodZ homologue SCO5751. pKT25-zip/pUT18c-zip represent the positive control. As a negative control, BTH101 carrying the empty vector plasmids pKT25 and pUT18c was used.

lation, *mreB* also was transcribed in vegetatively growing mycelium. This indicates that besides its function in directing spore wall synthesis, MreB has an additional role in vegetatively growing mycelium under certain conditions. The *mreB* RT-PCR data are in agreement with previous reports by S1 mapping experiments that identified three promoters, one strongly induced during sporulation (6). Interestingly, the −35 and −10 regions (GGAAC-N_{17}-CGTCCTC) of the *mreB* P1 promoter (6) closely resemble σ^E-dependent promoters (GCAAC-N_{17}-CGTCTTC) (23), suggesting the transcription of P1 by SigE and therefore the induction of *mreB* by cell wall stress. σ^E is part of a signal transduction system sensing certain changes in the integrity of the cell envelope (24) and transcribing the *cwg* operon putatively involved in cell wall glycan synthesis (23). The phenotype of a σ^E mutant, with an altered cell wall structure and increased sensitivity to cell wall-lytic enzymes, resembled somewhat that of the Δ*mreB* mutant (37, 39). However, whereas the Δ*mreB* mutant had an impaired spore wall, the *sigE* mutants suffered from a defective cell wall during vegetative growth (39).

The phenotype of the Δ*mbl* mutant closely resembled that of Δ*mreB*, with swollen prematurely germinating spores that had lost their resistance to detrimental environmental conditions, such as heat, detergents, and salt stress. This clearly indicated that Mbl and MreB cooperate in directing the synthesis of a stress-resistant spore wall, and that both are necessary for this process. Interestingly, Δ*mbl* and Δ*mreB* spores showed a different behavior when exposed to cell wall-lytic agents. Whereas spore germination in the Δ*mreB* strain was highly sensitive to lysozyme and vancomycin, Δ*mbl* spores were almost as resistant as the wild type, revealing a less crucial role for Mbl. The localization of *mreB* in the same gene cluster as that of *pbp2*, encoding a monofunctional transpeptidase, allows speculation on the defect leading to the impaired spore wall of the Δ*mreB* mutant and its increased sensitivity. Due to the missing MreB filaments, PBP2 might not be positioned properly in relation to the spore periphery, causing the spore wall to be less cross-linked.

As previously shown for the Δ*mreB* mutant (37), Δ*mbl* also

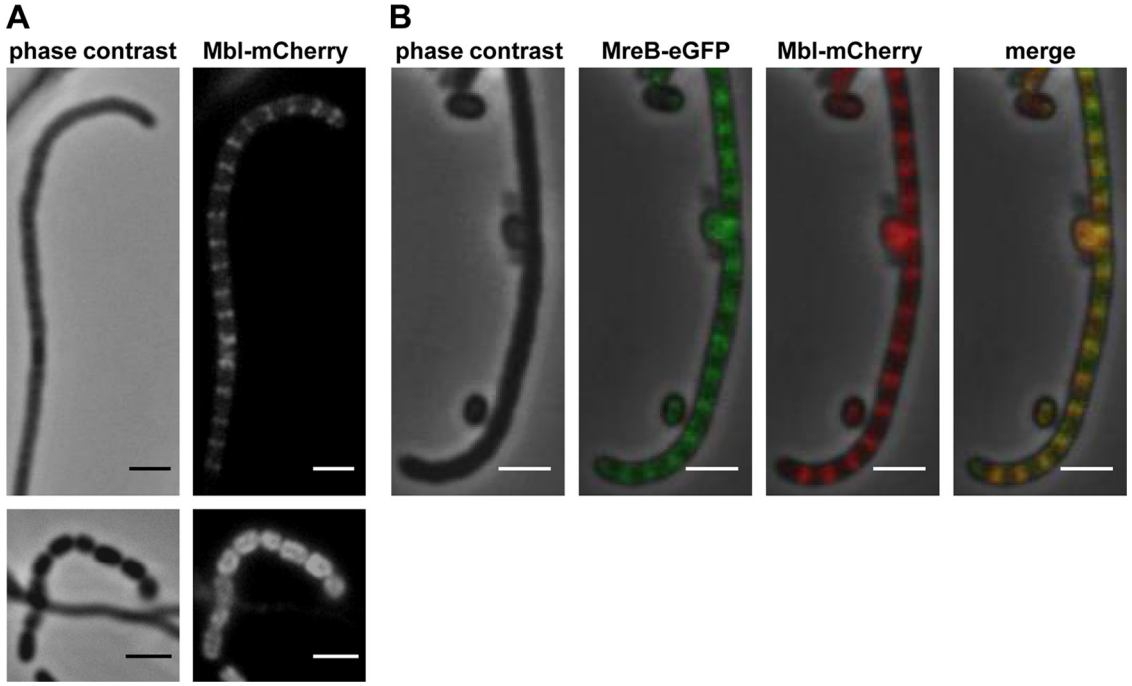

FIG. 6. Colocalization of Mbl and MreB to putative sporulation septa. (A) Plasmid pAH5 was integrated into the chromosomal *mbl* gene of *S. coelicolor* M145 via homologous recombination. The Mbl-mCherry fusion protein forms a ladder-like structure at putative sporulation septa and localizes around the cell periphery in young spores (bottom panels). (B) Colocalization of Mbl-mCherry and MreB-eGFP in the aerial mycelium. Plasmid pPM4 carrying a *mreB-egfp* fusion gene was integrated into the ΦC31 *att* site of M145::pAH5, generating M145::pAH5-pPM4. Bar, 2 μm.

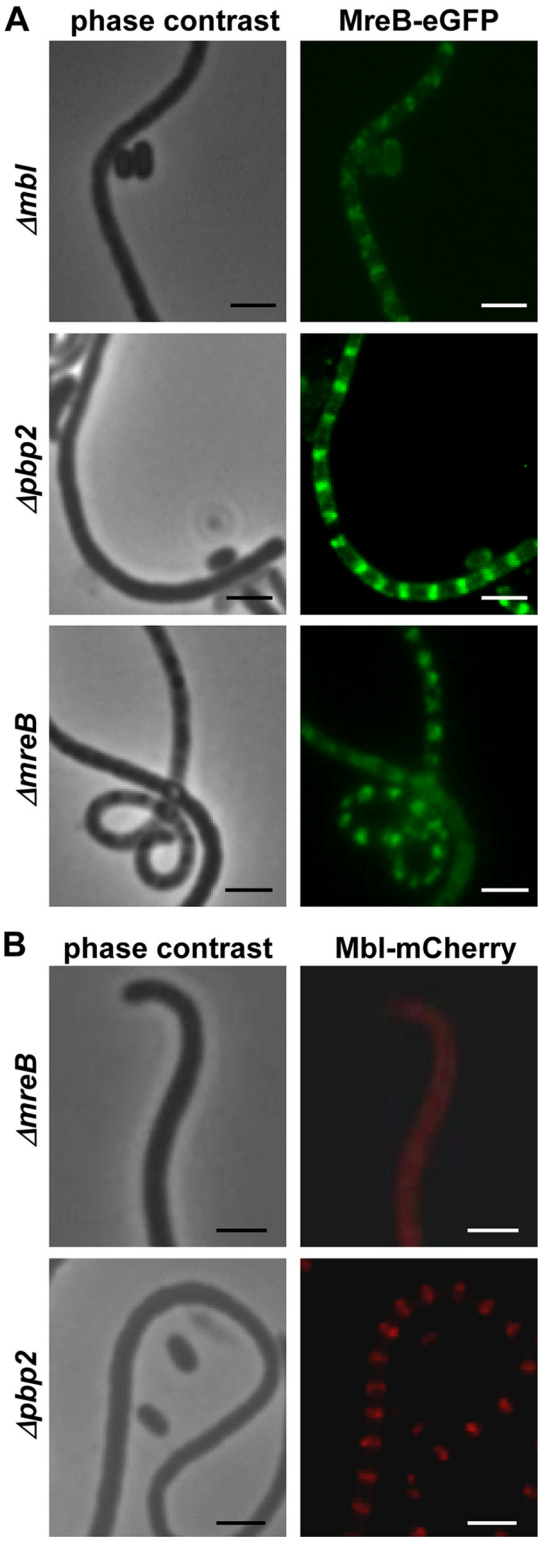

FIG. 7. Mbl-mCherry dependence on MreB for proper localization. The localization of MreB-eGFP and Mbl-mCherry was studied in Δ*mreB*, Δ*pbp2*, and Δ*mbl* mutants, which have similar morphological defects. (A) MreB-eGFP localizes to the sporulation septa even in the absence of Mbl or PBP2. (B) While the localization of Mbl-mCherry was not affected in the Δ*pbp2* mutant, it was unable to localize to the sporulation septa in the Δ*mreB* mutant, suggesting that Mbl depends on the presence of MreB for proper localization. Bar, 2 μm.

had a distorted spore wall. Whereas wild-type spores are ellipsoid with a sharply visible external wall, electron microscopic images showed irregularly shaped Δ*mbl* spores with a more diffuse wall (see Fig. S4 in the supplemental material). Since the Δ*mbl* spores are sensitive to many treatments, we cannot exclude that the appearance of the spore surface is affected by the fixation/staining process.

MreB localized to the sporulation septa and the spore periphery even in the absence of Mbl. It also localized properly in a Δ*pbp2* mutant, which showed the same morphological defects as those of the Δ*mreB* and Δ*mbl* mutants (30a). Also, MreB of *Caulobacter crescentus* was able to form normal helical spirals in MreC-depleted cells (15). In contrast, a distorted MreB localization pattern was observed in *E. coli* MreC-, MreD-, and RodA-depleted cells (32). Mbl, however, seems to rely on the presence of MreB filaments. While Mbl-eGFP or Mbl-mCherry properly localized at the sporulation septa in M145 or Δ*pbp2*, no clear Mbl-mCherry fluorescence foci were observed in the Δ*mreB* mutant.

Although MreB and Mbl seem to cooperate in spore wall synthesis, MreB has a more important role than Mbl. This also is supported by the protein-protein interaction studies that showed the strong interaction of MreB with RodZ, which probably represents the main scaffold protein for the peptidoglycan-synthesizing complex (1, 19, 49).

SCO6166 has a nonessential role during vegetative growth. SCO6166 differs in many aspects from the other MreB homologues. Whereas homology modeling revealed a highly similar structure for MreB and Mbl, SCO6166 lacks subdomains IB and IIB of actin-like proteins. Deviations in the IB and IIB subdomains from MreB and actins also are displayed by ParM, which is involved in plasmid partitioning, and this was proposed to influence the structure of the respective filaments (50).

The localization of *sco6166* in an operon with *sco6165* and their translational coupling suggest that both proteins cooperate. SCO6165 is homologous to DksA, a suppressor of DnaK. This suggests a function of SCO6165/SCO6166 in heat shock or stress response. Although many *Streptomyces* strains encode an SCO6165/SCO6166 pair, several *Streptomyces* strains without an SCO6166 homologue also exist, indicating an ancillary function of SCO6165/SCO6166.

In contrast to *mreB* and *mbl*, which are induced during morphological differentiation, *sco6166* had a completely different expression profile, being highly expressed in vegetative mycelium but completely switched off during sporulation. The RT-PCR experiments are in agreement with fluorescence microscopy studies, which detected SCO6166-mCherry only in substrate mycelium and not in aerial mycelium or spores. This clearly indicates a role of SCO6166 during vegetative growth and not in sporulation.

In summary, we showed that the three MreB proteins of *S. coelicolor* have distinct functions. MreB and Mbl are involved in the synthesis of a stress-resistant spore wall, with MreB probably providing a scaffold for the assembly of Mbl filaments. The role of SCO6166 during vegetative growth still is unclear and remains to be elucidated.

ACKNOWLEDGMENTS

We thank D. Ladant for providing the bacterial two-hybrid system, C. Menzel for help with TEM analyses, and K. Nieselt for providing microarray data.

The DFG (SFB766) provided financial support.

REFERENCES

1. **Alyahya, S. A., et al.** 2009. RodZ, a component of the bacterial core morphogenic apparatus. Proc. Natl. Acad. Sci. U. S. A. **106:**1239–1244.
2. **Bennett, J. A., et al.** 2009. Medium-dependent phenotypes of *Streptomyces coelicolor* with mutations in *ftsI* or *ftsW*. J. Bacteriol. **191:**661–664.
3. **Berman, H. M., et al.** 2000. The Protein Data Bank. Nucleic Acids Res. **28:**235–242.
4. **Bork, P., C. Sander, and A. Valencia.** 1992. An ATPase domain common to prokaryotic cell cycle proteins, sugar kinases, actin, and hsp70 heat shock proteins. Proc. Natl. Acad. Sci. U. S. A. **89:**7290–7294.
5. **Bullock, W. O., J. M. Fernandez, and M. J. Short.** 1987. X-L1blue, a high efficiency plasmid transforming *recA Escherichia coli* strain with beta galactosidase selection. Biotechniques **5:**376–378.
6. **Burger, A., K. Sichler, G. Kelemen, M. Buttner, and W. Wohlleben.** 2000. Identification and characterization of the mre gene region of *Streptomyces coelicolor* A3(2). Mol. Gen. Genet. **263:**1053–1060.
7. **Carballido-López, R.** 2006. The bacterial actin-like cytoskeleton. Microbiol. Mol. Biol. Rev. **70:**888–909.
8. **Carballido-López, R., et al.** 2006. Actin homolog MreBH governs cell morphogenesis by localization of the cell wall hydrolase LytE. Dev. Cell **11:**399–409.
9. **Cherepanov, P. P., and W. Wackernagel.** 1995. Gene disruption in *Escherichia coli*: TcR and KmR cassettes with the option of Flp-catalyzed excision of the antibiotic-resistance determinant. Gene **158:**9–14.
10. **Daniel, R. A., and J. Errington.** 2003. Control of cell morphogenesis in bacteria: two distinct ways to make a rod-shaped cell. Cell **113:**767–776.
11. **Defeu Soufo, H. J., and P. L. Graumann.** 2004. Dynamic movement of actin-like proteins within bacterial cells. EMBO Rep. **5:**789–794.
12. **Defeu Soufo, H. J., and P. L. Graumann.** 2005. *Bacillus subtilis* actin-like protein MreB influences the positioning of the replication machinery and requires membrane proteins MreC/D and other actin-like proteins for proper localization. BMC Cell Biol. **6:**10.
13. **Defeu Soufo, H. J., et al.** 2010. Bacterial translation elongation factor EF-Tu interacts and colocalizes with actin-like MreB protein. Proc. Natl. Acad. Sci. U. S. A. **107:**3163–3168.
14. **Divakaruni, A. V., C. Baida, C. L. White, and J. W. Gober.** 2007. The cell shape proteins MreB and MreC control cell morphogenesis by positioning cell wall synthetic complexes. Mol. Microbiol. **66:**174–188.
15. **Dye, N. A., Z. Pincus, J. A. Theriot, L. Shapiro, and Z. Gitai.** 2005. Two independent spiral structures control cell shape in *Caulobacter*. Proc. Natl. Acad. Sci. U. S. A. **102:**18608–18613.
16. **Errington, J.** 2003. Dynamic proteins and a cytoskeleton in bacteria. Nat. Cell Biol. **5:**175–178.
17. **Figge, R. M., A. V. Divakaruni, and J. W. Gober.** 2004. MreB, the cell shape-determining bacterial actin homologue, co-ordinates cell wall morphogenesis in *Caulobacter crescentus*. Mol. Microbiol. **51:**1321–1332.
18. **Formstone, A., and J. Errington.** 2005. A magnesium-dependent *mreB* null mutant: implications for the role of *mreB* in *Bacillus subtilis*. Mol. Microbiol. Mar;. **55:**1646–1657.
19. **Gerdes, K.** 2009. RodZ, a new player in bacterial cell morphogenesis. EMBO J. **28:**171–172.
20. **Guex, N., and M. C. Peitsch.** 1997. SWISS-MODEL and the Swiss-Pdb-Viewer: an environment for comparative protein modeling. Electrophoresis **18:**2714–2723.
21. **Gust, B., G. L. Challis, K. Fowler, T. Kieser, and K. F. Chater.** 2003. PCR-targeted *Streptomyces* gene replacement identifies a protein domain needed for biosynthesis of the sesquiterpene soil odor geosmin. Proc. Natl. Acad. Sci. U. S. A. **100:**1541–1546.
22. **Hempel, A. M., S. B. Wang, M. Letek, J. A. Gil, and K. Flardh.** 2008. Assemblies of DivIVA mark sites for hyphal branching and can establish new zones of cell wall growth in *Streptomyces coelicolor*. J. Bacteriol. **190:**7579–7583.
23. **Hong, H. J., M. S. Paget, and M. J. Buttner.** 2002. A signal transduction system in *Streptomyces coelicolor* that activates the expression of a putative cell wall glycan operon in response to vancomycin and other cell wall-specific antibiotics. Mol. Microbiol. **44:**1199–1211.
24. **Hutchings, M. I., H. J. Hong, E. Leibovitz, I. C. Sutcliffe, and M. J. Buttner.** 2006. The sigma(E) cell envelope stress response of *Streptomyces coelicolor* is influenced by a novel lipoprotein, CseA. J. Bacteriol. **188:**7222–7229.
25. **Jones, L. J., R. Carballido-Lopez, and J. Errington.** 2001. Control of cell shape in bacteria: helical, actin-like filaments in *Bacillus subtilis*. Cell **104:**913–922.
26. **Karimova, G., J. Pidoux, A. Ullmann, and D. Ladant.** 1998. A bacterial two-hybrid system based on a reconstituted signal transduction pathway. Proc. Natl. Acad. Sci. U. S. A. **95:**5752–5756.
27. **Kawai, Y., K. Asai, and J. Errington.** 2009. Partial functional redundancy of MreB isoforms, MreB, Mbl and MreBH, in cell morphogenesis of *Bacillus subtilis*. Mol. Microbiol. **73:**719–731.
28. **Kawai, Y., R. A. Daniel, and J. Errington.** 2009. Regulation of cell wall morphogenesis in *Bacillus subtilis* by recruitment of PBP1 to the MreB helix. Mol. Microbiol. **71:**1131–1144.
29. **Kieser, T., M. J. Bibb, M. J. Buttner, K. F. Chater, and D. A. Hopwood.** 2000. Practical *Streptomyces* genetics. The John Innes Foundation, Norwich, CT.
30. **Kim, S. Y., Z. Gitai, A. Kinkhabwala, L. Shapiro, and W. E. Moerner.** 2006. Single molecules of the bacterial actin MreB undergo directed treadmilling motion in *Caulobacter crescentus*. Proc. Natl. Acad. Sci. U. S. A. **103:**10929–10934.

30a. **Kleinschnitz, E.-M., A. Heichlinger, K. Schirner, J. Winkler, A. Latus, I. Maldener, W. Wohlleben, and G. Muth.** 18 January 2011. Proteins encoded by the *mre* gene cluster in *Streptomyces coelicolor* A3(2) cooperate in spore wall synthesis. Mol. Micorbiol. doi:10.1111/j.1365-2958.2010.07529.x. [Epub ahead of print.]

31. **Kruse, T., et al.** 2006. Actin homolog MreB and RNA polymerase interact and are both required for chromosome segregation in *Escherichia coli*. Genes Dev. **20:**113–124.
32. **Kruse, T., J. Bork-Jensen, and K. Gerdes.** 2005. The morphogenetic MreBCD proteins of *Escherichia coli* form an essential membrane-bound complex. Mol. Microbiol. **55:**78–89.
33. **Kruse, T., and K. Gerdes.** 2005. Bacterial DNA segregation by the actin-like MreB protein. Trends Cell Biol. **15:**343–345.
34. **Kruse, T., J. Moller-Jensen, A. Lobner-Olesen, and K. Gerdes.** 2003. Dysfunctional MreB inhibits chromosome segregation in *Escherichia coli*. EMBO J. **22:**5283–5292.
35. **Letek, M., et al.** 2008. DivIVA is required for polar growth in the MreB-lacking rod-shaped actinomycete *Corynebacterium glutamicum*. J. Bacteriol. **190:**3283–3292.
36. **MacNeil, D. J., et al.** 1992. Analysis of *Streptomyces avermitilis* genes required for avermectin biosynthesis utilizing a novel integration vector. Gene **111:**61–68.
37. **Mazza, P., et al.** 2006. MreB of *Streptomyces coelicolor* is not essential for vegetative growth but is required for the integrity of aerial hyphae and spores. Mol. Microbiol. **60:**838–852.
38. **Nieselt, K., et al.** 2010. The dynamic architecture of the metabolic switch in *Streptomyces coelicolor*. BMC Genomics **11:**10.
39. **Paget, M. S., L. Chamberlin, A. Atrih, S. J. Foster, and M. J. Buttner.** 1999. Evidence that the extracytoplasmic function sigma factor sigmaE is required for normal cell wall structure in *Streptomyces coelicolor* A3(2). J. Bacteriol. **181:**204–211.
40. **Pridmore, R. D.** 1987. New and versatile cloning vectors with kanamycin-resistance marker. Gene **56:**309–312.
41. **Redenbach, M., et al.** 1996. A set of ordered cosmids and a detailed genetic and physical map for the 8 Mb *Streptomyces coelicolor* A3(2) chromosome. Mol. Microbiol. **21:**77–96.
42. **Sali, A., and T. L. Blundell.** 1993. Comparative protein modelling by satisfaction of spatial restraints. J. Mol. Biol. **234:**779–815.
43. **Sambrook, J., and D. W. Russel.** 2001. Molecular cloning: a laboratory manual. Cold Spring Harbor Laboratory Press, New York, NY.
44. **Schirner, K., and J. Errington.** 2009. Influence of heterologous MreB proteins on cell morphology of *Bacillus subtilis*. Microbiology **155:**3611–3621.
45. **Söding, J., A. Biegert, and A. N. Lupas.** 2005. The HHpred interactive server for protein homology detection and structure prediction. Nucleic Acids Res. **33:**W244–W248.
46. **Tiffert, Y., et al.** 2008. The *Streptomyces coelicolor* GlnR regulon: identification of new GlnR targets and evidence for a central role of GlnR in nitrogen metabolism in actinomycetes. Mol. Microbiol. **67:**861–880.
47. **Tiyanont, K., et al.** 2006. Imaging peptidoglycan biosynthesis in *Bacillus subtilis* with fluorescent antibiotics. Proc. Natl. Acad. Sci. U. S. A. **103:**11033–11038.
48. **van den Ent, F., L. A. Amos, and J. Lowe.** 2001. Prokaryotic origin of the actin cytoskeleton. Nature **413:**39–44.
49. **van den Ent, F., C. M. Johnson, L. Persons, P. de Boer, and J. Lowe.** 2010. Bacterial actin MreB assembles in complex with cell shape protein RodZ. EMBO J. **29:**1081–1090.
50. **van den Ent, F., J. Moller-Jensen, L. A. Amos, K. Gerdes, and J. Lowe.** 2002. F-actin-like filaments formed by plasmid segregation protein ParM. EMBO J. **21:**6935–6943.
51. **Vollmer, W., and S. J. Seligman.** 2010. Architecture of peptidoglycan: more data and more models. Trends Microbiol. **18:**59–66.